Net ecosystem fluxes and composition of biogenic volatile organic compounds over a maize field–interaction of meteorology and phenological stages

FELIX WIß[1],*, ANDREA GHIRARDO[2],*, JÖRG-PETER SCHNITZLER[2] iD, CLAAS NENDEL[3], JÜRGEN AUGUSTIN[4] iD, MATHIAS HOFFMANN[5] and RÜDIGER GROTE[1] iD

[1]Karlsruhe Institute of Technology, Institute of Meteorology and Climate Research – Atmospheric Environmental Research (KIT/IMK-IFU), Garmisch-Partenkirchen, Germany, [2]Helmholtz Zentrum München, Institute of Biochemical Plant Pathology, Research Unit Environmental Simulation (EUS), Neuherberg, Germany, [3]Leibniz Centre for Agricultural Landscape Research (ZALF), Institute of Landscape Systems Analysis, Müncheberg, Germany, [4]Leibniz Centre for Agricultural Landscape Research (ZALF), Institute of Soil Landscape Research, Müncheberg, Germany, [5]Leibniz Centre for Agricultural Landscape Research (ZALF), Institute of Landscape Biogeochemistry, Müncheberg, Germany

Abstract

Bioenergy crop production is rapidly expanding in Europe, and the potential emissions of biogenic volatile organic compounds (BVOCs) might change the chemical composition of the atmosphere, influencing in turn air quality and regional climate. The environmental impacts of bioenergy crops on air chemistry are difficult to assess due to a lack of accurate field observations. Therefore, we studied BVOC fluxes from a bioenergy maize field in North-Eastern Germany throughout the entire reproductive growth stage of the plants. Combining automated large chambers and proton transfer reaction mass spectrometry (PTR-MS), we successfully measured fluxes of the highly reactive hydrocarbons monoterpenes (MTs) and sesquiterpenes (SQTs), together with several other BVOCs, including alcohols, aldehydes, ketones, benzenoids, and fatty acid derivatives. Emissions of MTs and SQTs were relatively high (17.0% and 3.6% of total mean molar BVOC emission, respectively) compared to methanol emissions (17.6%). Seasonal MT and SQT fluxes were clearly associated with the flowering phase, originating mainly from the flowering tissues as shown in additional laboratory experiments. From the observations of CO_2 net ecosystem exchange and evapotranspiration rates, we could exclude heat and drought stress-induced BVOC emissions. Standard emission factors calculated for all compounds, chemical groups, and growth stages, showed that the temperature dependency of volatile terpenoid fluxes decreased distinctively with proceeding development stage. The results indicate that emissions from large-scale bioenergy maize fields should be better differentiated and considered in regional estimates of aerosol formation. For the implementation of such relation into biogeochemical modelling, it should be considered that not only seasonal weather development but also phenological growth stages are determining the BVOC patterns and emission potentials.

Introduction

Biogenic volatile organic compounds (BVOCs) play a pivotal role for air chemistry processes and the formation of secondary organic aerosols (SOA). They increase CH_4 life time by removing hydroxyl radicals, participate in the formation of SOA, and are essential for photochemical ozone production (Atkinson & Arey, 2003;

Makkonen *et al.*, 2012; Calfapietra *et al.*, 2013; Schultz *et al.*, 2015). Thus, BVOCs affect air quality and (by affecting radiation extinction and cloud formation) also regional climate. BVOC emissions strongly depend on plant species and on environmental conditions that are all subject to change, in particular temperature, radiation, and water availability (Kesselmeier & Staudt, 1999). Thus, the effects of a changed BVOCs emission regime related to major land-use changes should not be neglected (Rosenkranz *et al.*, 2015).

In many parts of the world, especially in the tropics, bioenergy production is currently one of the largest drivers of land-use change (Rosenkranz *et al.*,

*These authors equally contributed to this work.

Correspondence: Rüdiger Grote, tel. ++49 8821 183 124, fax ++49 8821 183 247, e-mail: ruediger.grote@kit.edu

2015). Biomass is already the main contributor to total primary renewable energy supply. For Germany, this share is about 57% (in 2015), while it is even higher for whole Europe (62% in 2012) or at the global scale (72% in 2013) (European Union, 2014; International Energy Agency, 2015; Fachagentur für Nachwachsende Rohstoffe, 2016). Until 2050, projections for the EU show a further increase of biomass and waste usage for total primary energy production from currently 136 Mt oil equivalents to 164 Mt (Capros *et al.*, 2014). Also Germany has set goals to increase the fraction of renewable energy sources from currently 13% up to 50% using 26% of total primary energy supply from biomass (Erneuerbare-Energien-Gesetz, 2014; Arbeitsgemeinschaft Energiebilanzen, 2015). Apart from direct biomass burning, fermentation into biogas is a main energy production pathway, with currently maize as a preferred substrate (Fachagentur für Nachwachsende Rohstoffe, 2016). Maize, along with rapeseed, energy grasses or poplar and willow coppices, is supposed to play an important role in future agricultural production of renewable energy (Bentsen & Felby, 2012). This development has raised environmental concerns, in particular related to groundwater pollution (Nikièma *et al.*, 2012), additional greenhouse gas releases (Crutzen *et al.*, 2008), or biodiversity issues (Immerzeel *et al.*, 2014). However, changes in the emission regimes of BVOCs caused by land-use change have received not much attention so far (Rosenkranz *et al.*, 2015).

In the US, the high-emitting giant cane (*Arundo donax* L.) has been evaluated having a negative impact on air quality when extensively planted (Porter *et al.*, 2012), while a land-use change from natural to energy grasses, which are supposed to be low emitters, may have contrary impacts (Miresmailli *et al.*, 2013). For the majority of bioenergy plants such as rapeseed, however, the impact of BVOCs on air quality is generally seen as smaller (Morrison *et al.*, 2016) or indifferent from other agricultural crops (Renner & Münzenberg, 2003). In Europe, the air quality impacts of a changed BVOCs emission regime have only been considered yet in case of extended short rotation coppices with hybrid poplars (Ashworth *et al.*, 2013; Beltman *et al.*, 2013) which are well-known as high BVOC emitters, but do play only a minor role in current crop cultivation (∼1 ‰ of the total agricultural area in Germany). Nonetheless, the few studies addressing BVOC emissions from maize fields show large qualitatively and quantitatively discrepancies, due to different methodologies ranging from field leaf-level flux analysis to concentration gradient measurements and eddy covariance technique. Often, measurements were taken manually at midday for few days, carried out for leaves only or are concentrating on

early growth stages (Das *et al.*, 2003; Graus *et al.*, 2013; Leppik *et al.*, 2014). Only Bachy *et al.* (2016) reported field fluxes over an entire growing season by means of using eddy covariance. Thus, the BVOC fluxes known so far differ strongly, although the most abundant documented fluxes were methanol followed by monoterpenes (MTs), acetone, and green leaf volatiles (GLVs; for more details see Brilli *et al.*, 2011). Remarkably, sesquiterpene (SQT) fluxes have not been described under field conditions so far, probably due to technical and methodological difficulties, although these highly reactive compounds are assumed playing an important role in air chemistry regarding aerosol formation (Bonn & Moortgat, 2003).

In this study, we analysed changes of BVOC emissions from a maize field as a function of environmental cofactors, phenological stages, and plant status (potential heat and drought stress effects). To achieve this, we applied large automatic chamber systems, initially used to capture net ecosystem exchange (NEE) of CO_2 and evapotranspiration (Hoffmann *et al.*, 2016). These systems allow measuring concentration differences of air chemical compounds under almost all weather conditions and the simultaneously derived carbon and water fluxes can be used to evaluate plant stress. In contrast to eddy systems, large chambers capture fluxes for a specific plot only enabling to define precise boundary conditions without advective influences. We used these chambers for the first time in combination with proton transfer reaction quadrupole mass spectrometry (PTR-QMS) and infrared spectroscopy. In addition, we performed laboratory and greenhouse measurements determining tissue-specific BVOC emission pattern under controlled environmental conditions.

Overall we aimed to (i) examine the BVOC composition and fluxes throughout the major part of maize development, (ii) determine tissue-specific emissions, and (iii) evaluate the impact of environmental and phenological conditions on the source strength of BVOC emissions. Based on these data we calculated standard emission factors for the different plant growth stages, as prerequisite for accurate BVOC emission modelling of bioenergy maize fields.

Materials and methods

Description of the field site

The field study was conducted from the end of July until mid-September 2015 at the CarboZALF-D experimental site located at a ground moraine landscape near Dedelow, NE Germany (N 53.3793, E 13.7856) (Sommer *et al.*, 2016). Maize (*Zea mays* cv. Zoey, an energy and food cultivar from Advanta Seeds DMCC) was seeded at the end of April 2015 and harvested at 14

September 2015. The 690 m^2 parcel with 11 maize plants per m^2 and a row width of 0.75 m was neighboured by winter wheat and grassland. The site is equipped with instrumentation for greenhouse gas (GHG) flux analysis (i.e. CO_2, CH_4, and H_2O; Los Gatos Fast Greenhouse Gas Analyser; 9110010, Los Gatos), meteorological parameters (temperature, radiation, wind, relative humidity, atmospheric pressure) and soil temperature. The leaf area index (LAI) was measured at 5 cm height, six times for each of three directions to get one data point (SunScan Canopy Analysis Systm SS1-BF5, Delta-T, Cambridge, UK). LAI and aboveground biomass were determined at the beginning, mid, and end of the measurement period. The phenological growth stages of the maize plants were recorded each week and reported according to the Biologische Bundesanstalt, Bundessortenamt and Chemical industry (BBCH) identification keys (Meier, 2001).

Measurements of gas exchange and BVOCs in the field

BVOC fluxes were measured from 24 July to 15 September, including one day after the maize was harvested. The air was sampled from a closed system (flow-through non-steady-state) which consisted of two transparent automatic polycarbonate (thickness of 2 mm; light transmission ∼70%) chambers of 1.5 m × 1.5 m × 2.5 m size each, with about 20 maize plants growing in each chamber. Chambers were built more than six months prior to the measurements to minimize sources of additional VOCs from the chamber material. A 3/2 way polytetraflouretylen (PTFE) valve for each automatic chamber switched between drawing air from the closed chamber to the BVOC measuring device and drawing air when the chamber was opened for flushing the tube. Around 10 L min^{-1} air flow was drawn from both systems at the same time and, except for the ∼70 mL min^{-1} used for BVOC analysis, the air was redirected back into the chambers. Two fans per chamber ensured homogeneous air mixing. To minimize the impact of the chambers on the plant growth and to ensure ambient environmental conditions, the chambers were kept open for 80% of the time (i.e. 48 min h^{-1}). The median change rates and its standard deviation during a closed chamber period (i.e., within 12 min) were 0.02 and 1.43 K for the chamber temperature, 6.28 and 79.20 ppmv for CO_2, and 1750 and 6078 ppmv for H_2O, respectively.

BVOC concentrations were measured online using high-sensitivity PTR-QMS (Ionicon Analytik GmbH, Innsbruck, Austria) (Lindinger et al., 1998). Operation of the instrument and calculation of BVOC concentration have been previously described (Ghirardo et al., 2010, 2011; Kreuzwieser et al., 2014). For this study, we set the drift tube at pressure of 2.2 mbar, a voltage of 600 V and a temperature of 60 °C, resulting in an E/N of 134 Td (E = the electric field strength, N = the gas number density; 1 Td = 10^{-17} V cm^2). The ions from the first water cluster (i.e. $H_2O(H_3O)^+$), the O_2^+ and the NO^+ were kept below 10%, 3%, and 0.2% of the primary hydronium ions (H_3O^+), respectively.

We measured 18 different BVOCs (see Table 1) throughout approximately one minute. The PTR-QMS was connected to the chambers with approximately 20 m 1/4″ PTFE tubes with

Table 1 Selected compounds measured, respective protonated molecular mass (m/z), molecular formula, and the dwell time for measuring each compound's concentrations in seconds

m/z	Measured compound	Abbreviation	Formula	Dwell time (s)
21	Hydronium ions	-	$H_3^{18}O^+$	0.2
33	Methanol	-	CH_5O^+	2
39	Water cluster	-	$H_3O(H_2^{18}O)^+$	1
45	Acetaldehyde	-	$C_2H_5O^+$	5
47	Ethanol	-	$C_2H_7O^+$	1
59	Acetone	-	$C_3H_7O^+$	1
69	Fragments of pentanal; Octanal; Nonanal; Decanal	m/z 69	-	5
71	Unspecified mass feature	m/z 71	-	1
99	(E)-2-hexenal; (Z)-3-hexenal	GLV*	$C_6H_{11}O^+$	2
01	(E)-2-hexenol; (Z)-2-hexenol; (E)-3-hexenol; (Z)-3-hexenol; hexanal	GLV*	$C_6H_{13}O^+$	2
107	Xylenes; Benzene; 1,2,3-trimethyl (fragment)	Xylenes	$C_8H_{11}^+$	1
137	Monoterpenes†	MT	$C_{10}H_{17}^+$	5
151	(E)-4,8-dimethyl-1,3,7-nonatriene	DMNT	$C_{11}H_{19}^+$	1
153	Camphor; (E)-2-caren-4-ol; Methyl salicylate 4-ethylguaiacol	m/z 153	$C_{10}H_{17}O^+$ $C_8H_9O_3^+$ $C_9H_{13}O_2^+$	5
155	Oxygenated monoterpenes†	oMT	$C_{10}H_{19}O^+$	1
205	Sesquiterpenes†	SQT	$C_{15}H_{25}^+$	10
225	$C_{13}H_{20}O_3/C_{17}H_{20}$	m/z 225	$C_{13}H_{21}O_3^+$, $C_{17}H_{21}^+$	1

*These lipoxygenase (LOX) products, commonly called green leaf volatiles (GLV) are fatty acids derivatives of the octadecanoid pathway (Ghirardo et al., 2011; Portillo-Estrada et al., 2015).
†See Table S1 for the chemical identification.

T-pieces and fittings all made of PTFE. To avoid condensations, the tubings were thermally isolated and heated with minimum 6 K above ambient temperature and a maximum of 40 °C of the tubing. Chemical identification of BVOCs was achieved off-line by collecting altogether 8.4 L of air in glass tubes containing polydimethylsiloxane (PDMS) foam (Gerstel, Mülheim an der Ruhr, Germany) and adsorbent material (Carbopack X) at a flow rate of 150 mL min^{-1} for 56 min. The samples were collected when chambers were closed, and control measurements were taken, when chambers were open. The sample tubes were transported to the laboratory and stored for few days at 4 °C prior to gas chromatography mass spectrometry (GC-MS) analysis. The analysis was achieved by thermo-desorption (TD) and GC-MS (GC type: 7890A; MS type: 5975C; both from Agilent Technologies, Palo Alto, CA, USA), as previously described in Ghirardo *et al.* (2012, 2016). The sampling was repeated at least 4 times and, compared to controls, only the BVOCs that significantly increased after closing the chambers were considered in further analyses. The TD-GC-MS data indicate negligible source of polycarbonate compounds originated from the chambers. In our study, the ions at mass to charge ratio (*m/z*) 69 and *m/z* 71 recorded by PTR-QMS were quantified as they were isoprene and methyl venyl ketone (MVK) + methacrolein (MACR) as commonly accepted in PTR-QMS measurements from vegetation (Hansel *et al.*, 1999). However, we were not able to confirm these molecules by TD-GC-MS analyses, which indicated that signals recorded at *m/z* 69 were possibly originating from a mixture of fragmentations of the fatty aldehydes pentanal, octanal, nonanal, and decanal, as the chemical noise possibly originating from the polycarbonate material was negligible. This should be taken into account when values of *m/z* 69 and 71 are reported in the following. The signal at *m/z* 153 reflected methyl salicylate, camphor, (*E*)-2-caren-4-ol, and 4-ethylguaiacol; the signal at *m/z* 225 $C_{17}H_{20}$ and $C_{13}H_{20}O_3$ (possibly methyl jasmonate). The proportion of compounds recorded at the same *m/z* could not be reliably determined. Therefore, data are presented referring to the *m/z* values. Fumigating chambers using a 11 VOC standard-mixture (Apel-Riemer Environmental, Denver, CO, USA) at 1 ppmv and constant air flow of 750 mL min^{-1} showed linear increasing of respective PTR-QMS *m/z* signals when the chambers were closed. At the end of the field study and after harvesting all plants, the PTR-QMS measurements recorded very low emissions of BVOCs from soil. Additionally, when the soil was covered with aluminium sheets, BVOC emissions were negligible. Thus it can be concluded that the material composition of the chambers did not significantly impact our measurements.

Laboratory experiment

BVOC samples were separately collected from roots (R), leaves (L), male flowers (F) (also called tassels) and emerged but not dried stigmata of the corn (S) (also called silk). In laboratory studies, these samples were analysed under environmentally controlled conditions to determine the origin of BVOCs measured during the field campaign. Plants from the same maize cultivar as grown outside were grown in the greenhouse of the Helmholtz Zentrum München, Neuherberg, Germany. Seeds were sown three times with a time lag of 4 weeks to obtain three different phenological stages at the time of measurement. According to the BBCH identification keys for maize, these growth stages can be described as leaf development (LD; half of all number of leaves unfolded), as the mid and as the end of the flowering phase (FW$_{MID}$ and FW$_{END}$, respectively). As flowering of the tassel and emerging of stigmata depends on the growth stage of the plant, BVOC analyses from those two compartments were carried out with plants in FW$_{MID}$. BVOC collections from roots were only measured in LD and FW$_{MID}$, as no significant changes appeared in the development of the root system between FW$_{MID}$ and FW$_{END}$. BVOC emissions were collected and analysed by TD-GC-MS using the same headspace sorptive extraction approach described previously in Weikl *et al.* (2016).

The different plant tissues were enclosed into transparent glass vials of 2-mL (for roots, flowers, and stigmata) and 10-mL volume (for leaves) with nonpolar, PDMS coated stir bars (Twister, film thickness 0.5 mm, Gerstel) and incubated for 65 h under light condition (photosynthetically active radiation (PAR) ~100 µmol m^{-2} s^{-1}). The mass of analysed roots was 536 ± 39 mg, of the flower 75 ± 15 mg, of the stigmata 188 ± 15 mg. Leaf discs of 4.9 cm^2 were punched from a leaf at two of three of the leaf length in respect to the stem but out of the midvein (L$_{M1}$), which represents the reference leaf among the different growth phases LD, FW$_{MID}$, and FW$_{END}$. To investigate the leaf-age dependency, additional leaf discs were collected from the same growth stage FW$_{MID}$: an upper leaf (L$_U$) which is younger than the reference leaf L$_{M1}$, a lower leaf (L$_L$) older than L$_{M1}$, and from the same leaf of L$_{M1}$ but at 1/3 of the leaf length (L$_{M2}$), therefore, closer to stem. Leaf discs were accommodated at the bottom of the 10 mL vial with 200 µL carbonated water (Aqua Culinaris Medium, Urstromquelle GmbH, Baruth/Mark, Germany) to continuously provide CO_2 for leaf photosynthesis. Control measurements were carried out exactly in the same way, but in absence of the leaf material and the mass signals recorded (negligible) were used for background correction.

Calculation of BVOC fluxes

We calculated the BVOC fluxes as the slope of a linear regression (ordinary least squares), fitted to the concentration measurement points over time obtained during 12 min of sampling from each closed chamber. All fluxes from nonsignificant linear regressions (H0: slope of regression line is zero; $P > 0.05$; that is, r < 0.60 for a two-tailed t distribution test with 12 data points) were set to zero. We scaled all flux rates from ppb s^{-1} ($d\text{VOC}_{\text{ppb}}/dt$) to nmol m^{-2} ground area s^{-1} ($d\text{VOC}_{\text{mol m}^{-2}}/dt$) by

$$\frac{d\text{VOC}_{\text{mol m}^{-2}}}{dt} = \frac{d\text{VOC}_{\text{ppb}}}{dt} * \frac{V_{\text{Ch}}}{A_{\text{Ch}} * V_m} \quad (1)$$

with V_{Ch} (5.625 m^3) is the volume, A_{Ch} (2.25 m^2) is the base area of the chamber, and V_m is the molar volume calculated by the ideal gas law. From the resulting twofold 12-minute mean emission rates per hour, we calculated hourly mean and daily mean emission rates. Positive and negative fluxes indicate net ecosystem emissions and deposition, respectively.

From hourly mean values (daytime and night-time), we calculated standard emission factors (SEF) indicating species-specific emissions scaled to the defined environmental standard conditions of PAR at 1000 µmol m^{-2} s^{-1} and 30 °C leaf temperature (Guenther *et al.*, 1993). During the field study, we only found 20 data points per compound that complied with these conditions. Thus, similar to Tarvainen *et al.* (2005) we fitted the SEF with all observed hourly mean values for each compound to the equations proposed by Guenther (1997) (see Eqns (2) and (3)) by curve fitting via the Levenburg–Marquardt algorithm with nonlinear least squares. For all compounds we used the temperature-dependent emission function:

$$E_{obs} = SEF * C_{TM} \qquad (2a)$$

$$C_{TM} = e^{(\beta(T-T_S))} \qquad (2b)$$

with E_{obs} (µmol m^{-2} h^{-1}) as the observed emission rate at temperature T (K), β (K^{-1}) as an empirical temperature coefficient which was either set to 0.09 (Guenther *et al.*, 1993; Guenther, 1997; Tarvainen *et al.*, 2005) or also statistically fitted, and T_S being the standard temperature (303.15 K).

As some volatiles show strong dependencies on temperature as well as radiation (e.g. isoprene, and in some plant species also MTs (Loreto *et al.*, 2000; Ghirardo *et al.*, 2010)), we additionally applied the following function to determine SEFs:

$$E_{obs} = SEF * \frac{\alpha C_{L1} L}{\sqrt{1 + \alpha^2 L^2}} * \frac{e^{\left(\frac{C_{T1}(T-T_S)}{RTT_S}\right)}}{C_{T3} + e^{\left(\frac{C_{T2}(T-T_M)}{RTT_S}\right)}} \qquad (3)$$

with L (µmol m^{-2} s^{-1}) as PAR, R (8.314 J K^{-1} mol^{-1}) is the ideal gas constant, and α (0.0027), C_{L1} (1.066), C_{T1} (95 000 J mol^{-1}), C_{T2} (230 000 J mol^{-1}), C_{T3} (0.961, that is, depending on α to set Eqn (3) at standard light and temperature conditions to the value of 1), and T_M (314 K) are empirical parameters given by Guenther (1997). For m/z 69 and MTs, using Eqn (3) could describe the field observations better than using Eqn (2).

As SEFs may change with growth stages (Monson *et al.*, 2012), we distinguished between the three temporal periods of flowering (FW; 27 July–16 August, N = 495), fruit development and ripening (FR; 18 August–13 September, N = 591), and the whole season (WS; 27 July–13 September, N = 1110). Additionally, we calculated a mean SEF for each group of compounds with same seasonal flux pattern by:

$$gSEF_{gram} = \sum_i SEF_{i,gram} \left(\frac{SEF_{i,mol}}{gSEF_{mol}}\right) \qquad (4)$$

with $gSEF_{gram}$ as the mean group SEF in µg m^{-2} (ground) h^{-1}, $SEF_{i,gram}$ as the SEF of each component i within a group in µg m^{-2} h^{-1}, $SEF_{i,mol}$ as the SEF of each component i within a group in nmol m^{-2} s^{-1}, and $gSEF_{mol}$ as the summed group SEF in nmol m^{-2} s^{-1}. This equation can be described as the summed up molar fraction of each compound's SEF to the group SEF multiplied by its mass SEF.

To evaluate the development of BVOC fluxes that originate from cumulative temperature and radiation conditions, we also calculated the seasonal development (SD) based on the respective MEGAN algorithms (Guenther *et al.*, 2006).

$$SD = C_{TM} + f_t C_l \frac{C_t}{C_{t30}} \qquad (5a)$$

$$C_{t30} = C_{T2} \frac{e^{(C_{T1}x_{30})}}{C_{T2} - C_{T1} * [1 - e^{(C_{T2}x_{30})}]} \qquad (5b)$$

$$x_{30} = \frac{\frac{1}{T_{opt}} - \frac{1}{T}}{R} \qquad (5c)$$

with f_t, C_l, C_t, and T_{opt} being the dynamically calculated modifiers for the emission potential that are calculated in dependence on light and temperature of the previous ten days as described in Guenther *et al.* (2006). SD is calculated in half-hourly time steps and averaged over the day for presentations. The normalized SD factor is daily SD divided by the largest daily SD obtained in the measured period.

Calculation of net ecosystem CO$_2$ fluxes

Fluxes for the net ecosystem CO$_2$ exchange (NEE; µmol C m^{-2} s^{-1}) were calculated according to the ideal gas law, equivalent to the calculation of the BVOC fluxes (Eqn 1). Data noise that originated from either turbulence or pressure fluctuation caused by chamber deployment or from increasing saturation and canopy microclimate effects was excluded by the application of a death-band of 5% to each measurement (Davidson *et al.*, 2002; Kutzbach *et al.*, 2007; Langensiepen *et al.*, 2012). Multiple data subsets based on a variable moving window with a minimum length of 4 min were generated for each measurement (Hoffmann *et al.*, 2015) and linearly fitted (ordinary least squares; Leiber-Sauheitl *et al.*, 2014; Leifeld *et al.*, 2011; Pohl *et al.*, 2015) to calculate the concentration change with time. Resulting multiple NEE fluxes per measurement (based on the moving window data subsets per measurement) were subsequently scrutinized by the following threshold criteria: (i) range of within-chamber air temperature less than ±1.5 K (R$_{eco}$ and NEE fluxes) and deviation of photosynthetic active radiation (PAR) less than ±20% of the average; (ii) significant regression slope ($P \leq 0.1$); and (iii) nonsignificant tests ($P > 0.1$) for normality (Lillifor's adaption of the Kolmogorov–Smirnov test), homoscedasticity (Breusch-Pagan test) and linearity of CO$_2$ concentration data. Calculated CO$_2$ fluxes that did not meet all threshold criteria were discarded. In cases of more than one flux per measurement meeting all exclusion criteria, the NEE flux with the steepest slope was chosen.

Statistical analyses

Principal component analyses (PCA) were performed using the software package SIMCA-P (v13.0.0.0, Umetrics, Umeå, Sweden) following established procedures (for details, see Ghirardo *et al.*, 2012, 2016; Weikl *et al.*, 2016). The results were validated by full cross-validation and if specified, significant at the 95–99.9% confidence interval. One-way ANOVA was carried out at significance levels of $\alpha < 5\%$, using the software package SIGMA-PLOT (v11.0, Systat Software Inc., San Jose, CA, USA) and the PYTHON LIBRARY SCIPY (v0.14).

Results

Meteorology, plant growth stages, NEE, and evapotranspiration

The months of July, August, and September 2015 were generally drier (−24 mm, −13%) and warmer (+1.3 °C) compared to the long-term mean observations from 1992 to 2015 at the field site in Dedelow. While July was slightly warmer but wetter, August was notably warmer (+3 °C) and drier (−23 mm, −50%) than the long-term mean. September 2015 was generally in line with long-term observations. Based on the meteorological data, we distinguish five phases of measurement periods: (i) late July with low daily mean temperatures (around 15 °C) and frequent precipitation events, (ii) first half of August with oscillating but high temperatures (>20 °C) and mostly dry weather (only few precipitation events with maximum daily sums of 5 mm), (iii) second half of August with slightly cooler temperatures but higher radiation in the first week followed by days with lower radiation, (iv) a short period beginning of September when temperatures sharply rise and decline within few days, and (v) the rest of the measurement campaign with cooler temperatures (12 to 16 °C) and moist conditions. This sectioning of weather data enabled comparing the composition and quantity of BVOC fluxes from the two-week hot period of phase 2 with those from rather long-term average temperature conditions of phase 3 and 5.

During phase 1, maize plants were in the vegetative growth and the inflorescence emerged; in phase 2 the plants were flowering and reached highest NEE and evapotranspiration rates; in phase 3 and 4 the fruit developed and during phase 5 the plants were ripening–according to the phenological growth stages from the BBCH identification keys of maize (Meier, 2001). As the biomass of the maize plants inside the chambers could only be measured at the time of harvesting, the biomass development was determined from plants close to the chambers. Generally, only very low pest infestation by corn borer (*Ostrinia nubilalis*) has been reported during the year (data not shown).

Field BVOC fluxes

The PTR-QMS measured BVOC concentrations within the headspace of a chamber during the period when the chamber was closed (e.g. m/z 153, see Fig. 1). For many compounds, no significant concentration changes during night had been observed indicating neither net ecosystem emission nor net deposition of BVOCs. This further indicates that the production of these compounds was strongly light-dependent. In the morning hours, concentrations of all emitted compounds slowly rise with maximum increases generally appearing
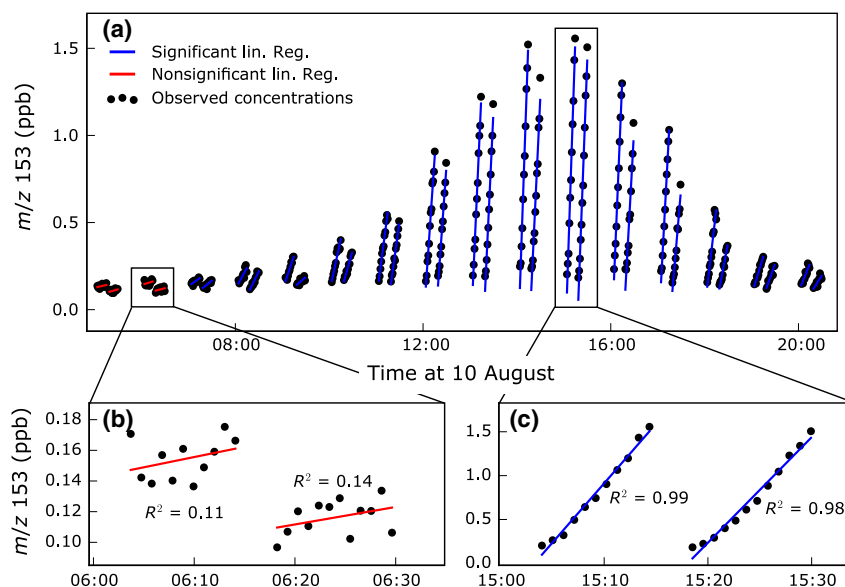

Fig. 1 Typically observed linear concentration increases of m/z 153 (sum of methyl salicylate, camphor, (*E*)-2-caren-4-ol, and 4-ethyl-guaiacol) within two automatic chamber headspaces during 10 August 2015. For each period of a closed chamber (approx. 12 min), the slope of a linear regression (fitted by ordinary least squares), indicated by blue ($P < 0.05$) and red lines ($P > 0.05$), corresponds to the emission rate in ppb 12 min^{-1}. (a) Entire diurnal cycle; (b) early morning nonsignificant concentration changes, (c) significant concentration changes during afternoon.

around early afternoon and then subsequently decreasing again. This diurnal cycle was temperature- and light-dependent, reaching emission maxima around early afternoon and minima in the night or during early morning hours (Fig. 2).

Absolute fluxes

Throughout the whole study, the highest daily mean BVOC emissions were observed within the 2nd phase (flowering and beginning of fruit development), when means of temperature and radiation were highest (Fig. 3c–e). Similar environmental conditions of temperature and radiation were observed in phase 4 ($P > 0.05$; ANOVA), but all BVOC emissions except for ethanol ($P = 0.051$) were significantly lower than in phase 2, suggesting that the plant phenology was a key factor in controlling BVOC emissions. We observed rather low BVOC fluxes during the end of the vegetative growth phase as well as during the end of the fruit development until plant ripening. The change in methanol flux from a net ecosystem emission to a net deposition was very likely caused by its high water solubility as it coincides with precipitation events (Niinemets *et al.*, 2004).

Overall, highest molar emissions (>0.20 nmol m^{-2} s^{-1}) were measured for GLVs, MTs, methanol, acetone, and acetaldehyde (arranged in decreasing order), with a corresponding mean portion to total molar BVOC emissions of 13.2% to 18.1% for the whole period (see Table 2). Lower molar emissions (<0.10 nmol m^{-2} s^{-1}) were measured for m/z 69, m/z 153, SQT, ethanol, and m/z 71 (arranged in decreasing order) with portions < 5.4% for the whole period. Very low but still significant emissions were detected for (*E*)-4,8-Dimethyl-1,3,7-

nonatriene (DMNT), xylenes, oxygenated MTs (oMTs), and a $C_{17}H_{20}/C_{13}H_{20}O_3$ compound (m/z 225) (not shown). Until harvesting (ripening growth stage) the emissions of most of the compounds gradually decreased to daily mean values below 0.03 nmol m^{-2} s^{-1}. At harvesting as well as on the following day, all emissions were below 0.01 nmol m^{-2} s^{-1}. We also observed net deposition fluxes of methanol and ethanol and to some degree also of acetaldehyde and acetone. Whereas mean compound emissions are decreasing with growth stage, the partitioning between the compounds is more complex (see Table 2), with some compounds increasing portions in later growth stages (GLVs, acetone, ethanol, xylenes, acetaldehyde, m/z 71, and DMNT).

Normalized fluxes

By normalizing daily mean BVOC fluxes to each compound's daily mean maximum of the whole season, we separated the compounds into three groups with distinct seasonal flux patterns. The first group mainly consists of volatile terpenoids (MTs, oMTs, SQTs) and their derivatives (m/z 153, m/z 225) (see Fig. 4a). The second group summarizes the C_1-C_2 alcohols methanol and ethanol (see Fig. 4b). Compounds from the third group are defined as other VOCs (see Fig. 4c) and include GLVs, acetaldehyde, m/z 71, xylenes, acetone, and DMNT, which originates from the terpenoid biosynthetic pathway (Richter *et al.*, 2016).

The volatile terpenoids show high fluxes particularly in phase 2 and then gradually decline. The methanol and ethanol fluxes showed emission and deposition rates with similar amplitudes and generally decreasing
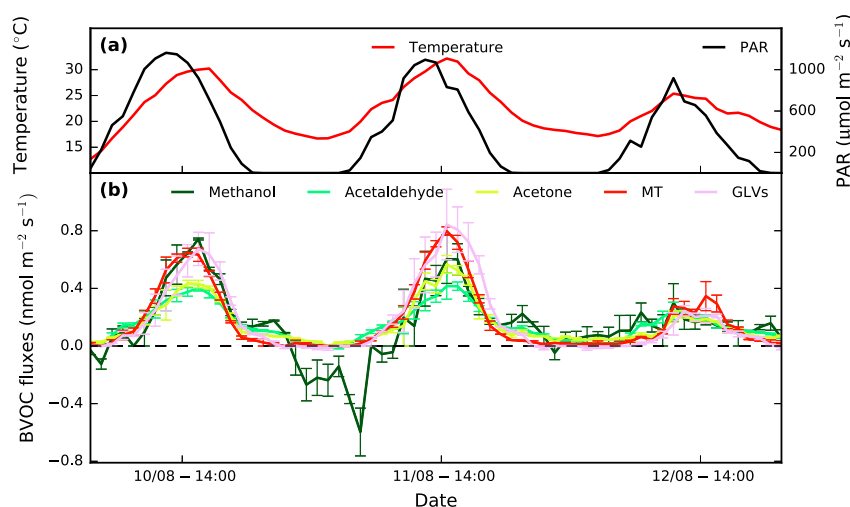

Fig. 2 Diurnal cycle of 10–12 August 2015. (a) Hourly mean temperature and photosynthetically active radiation (PAR); (b) hourly mean BVOC emission rates, with minimum and maximum values as error bars ($N = 2$).
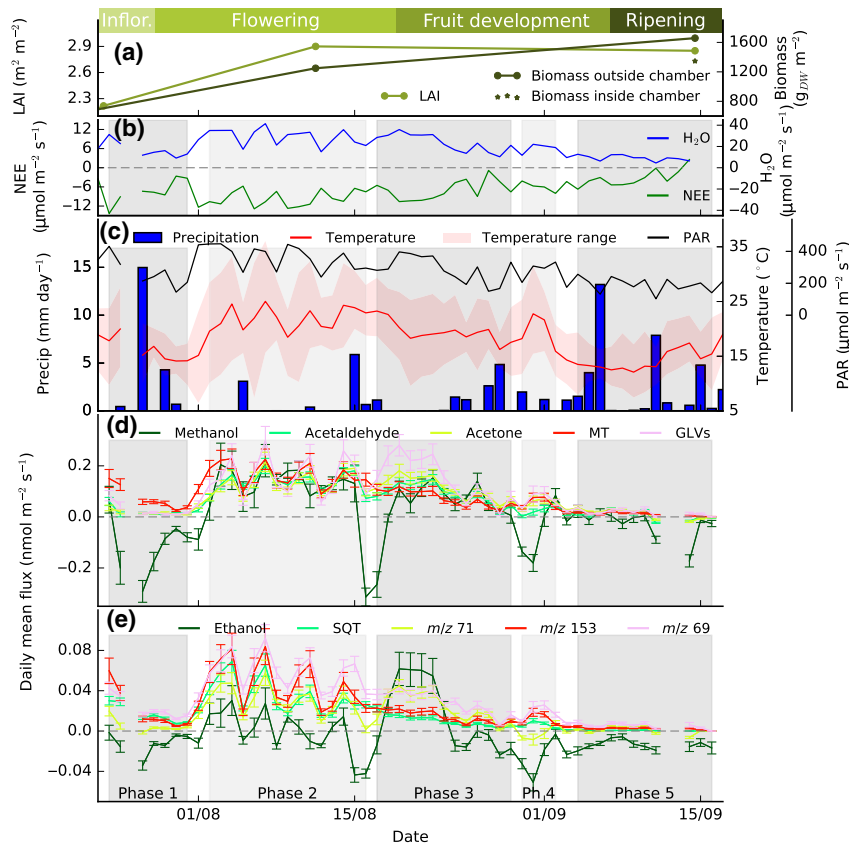
Fig. 3 (a) Phenological stages (Inflorescence emergence, Inflor.), leaf area index (LAI), plant biomass; (b) net ecosystem exchange (NEE), and evapotranspiration (H_2O; note the ×10 for a better comparison with NEE); (c) environmental conditions of precipitation (Precip), air temperature at 2 m aboveground, and photosynthetically active radiation (PAR); (d) most abundant BVOC fluxes; (e) less abundant BVOC fluxes from the maize ecosystem observed at CarboZALF field site in Dedelow 2015. The principal growth stages were observed on a weekly basis. Radiation, temperature, and BVOC fluxes ($N = 48$, means ± standard error) are shown as daily averages and precipitation as daily sums. Only daily values with more than 18 hours of data are shown. The meteorological phases described in the main text are depicted in grey and named in (e).

fluxes in phase 5. The group of other VOCs shows a similar flux pattern as terpenoids in phase 1 and 2 but did not decrease in phase 3. This group also showed a generally stronger oscillation of the emission rates until the end of phase 4. From the relation to the calculated SD development, it can be derived that terpenoid emissions considerably depend on past weather conditions (particularly apparent in phase 3), while the emissions of other VOCs strongly respond to instantaneous radiation and temperature. However, the emission increase in both groups at the start of phase 2 was generally more pronounced than indicated by the SD factor. Moreover, the responsiveness to the increase in temperature in phase 4 was much less than could be assumed from the cumulative weather conditions. Thus, cumulative weather as well as the development stage needs consideration to determine the correct emission pattern.

Tissue-specific BVOC emissions

The field measurements indicated that changes in terpenoid emissions could not be explained by environmental factors alone, suggesting that plant ontogenesis plays a crucial role for the pattern of overall plant emissions, especially for the steep increase of most compounds during the flowering phase. To determine the source of these emissions, we performed laboratory analyses under environmentally controlled conditions, measuring emission rates separately from different plant tissues and for different growth stages and leaf ages (Fig. 5b).

Overall, flowering tissues were the strongest source of terpenoids, in particular of oMTs, SQTs, and oxygenated SQTs (oSQTs), with up to 14-fold higher emission rates compared to leaves (see Fig. 5 and Table S1). Noteworthy, the BVOC emission rate of

Table 2 Mean molar emission in pmol m^{-2} s^{-1} (negative fluxes set to zero) and fraction of each compound to the total BVOC emission in % in brackets for the two phenological growth stages of flowering and the fruit development and ripening as well as for the whole observed growth period. See Table S1 for a further identification of the groups of MTs, oMTs, and SQTs

Compound	Flowering (21 days)	Fruit dev. and ripening (27 days)	Whole period (49 days)
Methanol	137.8 (17.6)	70.23 (16.2)	99.57 (16.8)
Acetaldehyde	102.12 (13.0)	57.65 (13.3)	78.05 (13.2)
Ethanol	12.94 (1.7)	16.65 (3.8)	14.98 (2.5)
Acetone	100.22 (12.8)	72.27 (16.7)	85.55 (14.4)
m/z 69	47.44 (6.1)	18.85 (4.4)	31.96 (5.4)
m/z 71	24.63 (3.1)	14.32 (3.3)	19.03 (3.2)
GLVs	122.5 (15.6)	93.59 (21.6)	107.78 (18.1)
Xylenes	9.89 (1.3)	9.42 (2.2)	9.73 (1.6)
MTs	133.46 (17.0)	49.19 (11.4)	87.96 (14.8)
DMNT	17.29 (2.2)	10.39 (2.4)	13.65 (2.3)
m/z 153	36.43 (4.7)	9.71 (2.2)	21.9 (3.7)
oMTs	9.56 (1.2)	4.47 (1.0)	6.84 (1.2)
SQTs	28.57 (3.6)	5.79 (1.3)	16.29 (2.7)
m/z 225	0.36 (0.0)	0.05 (0.0)	0.19 (0.0)
Total	**783.19 (100.0)**	**432.56 (100.0)**	**593.49 (100.0)**

Total sums are indicated in bold.

each compound varied significantly between the different plant tissues (ANOVA and PCA, see Fig. 5 and Table S1, respectively).

Moreover, corn stigmata also emitted relatively high rates of BVOCs, whereas in comparison, leaf and root emissions were rather small. Statistically significant increases in leaf emission were observed only for oSQT between the vegetative growth stage and the reproductive stage end of flowering ($P < 0.05$, ANOVA). Interestingly, the root system was a large source of 4-ethylguaiacol (m/z 153), a benzenoid derivative also emitted from the flowering tissues but not present in the bouquet of volatiles emitted from leaves. Principal component analysis indicated that limonene, 1,8-cineole, (E)-2-caren-4-ol, decanal, cyclosativene, β-cubebene, γ-cadinene, and β-sesquiphellandrene were strongly correlated to flowering tissue emissions, explaining 62% of the total data variance, when compared to emission rates from all the samples collected at different growth stages, leaf ages, and plant tissues (Fig. S1).

In summary, the laboratory analyses strongly indicated that the male flower and the stigmata acted as additional sources of terpenoids to the overall plant emissions. This is in line with observed fluxes in the field, where terpene emissions increased during the phase of flowering.

Changing standard emission factors under changing growth stages

Because it is scaled to specific environmental conditions, the SEF is independent from temperature and radiation, and therefore can be used to examine seasonal and phenological dependencies of BVOC emissions. Accordingly, we calculated SEFs for the different growth stages flowering (FW), fruit development together with ripening (FR), and the whole season (WS) (see Table 3). Highest SEFs (>40 µg m^{-2} h^{-1}) for WS were obtained for MT, GLVs, acetone, m/z 153, and SQT (arranged in decreasing order). The mean SEF for all terpenoids (from six BVOCs with 495, 591, and 1110 values each for FW, FR, and WS, respectively) decreases by half from FW to FR (114 to 60 µg m^{-2} h^{-1}). In contrast, the mean SEF for all other (seven) VOCs remains approximately constant at an emission rate around 54 µg m^{-2} h^{-1} for all seasons. The different SEF development is reasonably resembled by each specific compound within these two groups, except if an additionally influence of radiation is considered in the calculation of the SEFs. In this case, SEFs for MTs and m/z 69 only differed little between growth phases. The mean SEF value for methanol and ethanol is hardly meaningful as the SEF fit of the equation for temperature-dependent emissions with a constant β-coefficient of 0.09 was very poor for both alcohols ($R^2 < 0.2$).

When additionally fitting the β-coefficient, the standard error decreases with increasing R^2 for all compounds, meaning that the resulting function better represented the observed emission rates than only fitting the SEF value. For terpenoids and other VOCs this lead to a minimum β-coefficient of 0.131 K^{-1} for acetaldehyde during flowering and a maximum value of 0.203 K^{-1} for m/z 153 for the whole period.

Discussion

In the following, we discuss the changes and dependencies of BVOC fluxes from the investigated maize field throughout an almost entire growth period. In particular, we could show that flowering tissues are important additional sources of volatile terpenes. Nonterpene compounds did not show these phenological and seasonal dependencies but could be explained by instantaneous weather conditions. The application of a new technique that combines large automatic chambers with PTR-QMS technology showed the feasibility of measuring BVOC emissions at the field scale continuously over extended time periods. It also demonstrated that the total net carbon loss from all observed BVOCs during the field study (0.13 gC m^{-2}) was quite small in relation to the net carbon assimilation (561.1 gC m^{-2}). However,
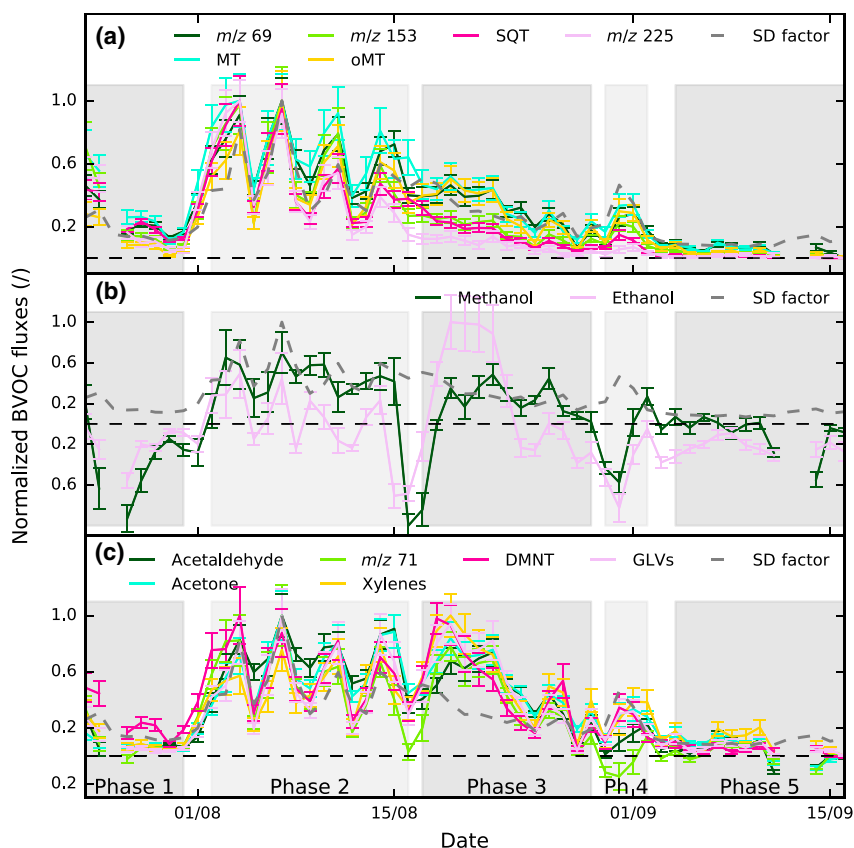
Fig. 4 Daily mean normalized BVOC emissions (emission rates scaled to each compound's maximum value throughout the measurement period) for all measured compounds. (a) group of mainly terpenoids and their derivatives; (b) group of methanol and ethanol; (c) group of other VOCs. The normalized simulated development (SD) factor calculated from cumulative temperature and radiation of the past ten days is also shown in each panel as a dashed grey line. The meteorological phases described in the main text are depicted in grey and named in (c) ($N = 48$, $\pm$ normalized standard error).

the emission of highly reactive MTs and especially SQTs in significant amounts indicates that maize fields are likely to play an important role in regional aerosol formation and should thus be considered in regional biosphere-atmosphere feedback analysis, particularly regarding land-use change scenarios that evaluate bioenergy production impacts.

Seasonality and phenology impact

The BVOC fluxes from the maize canopy were highly influenced by immediate temperature and radiation conditions. However, we also demonstrate an important impact of plant ontogenesis which is apparent from: (i) the very steep increase in MT, m/z 153, and SQT emissions during the flowering period (transition from meteorological phase 1 to 2) that could not be fully explained by current environmental conditions, (ii) the short period of temperature increase in late August/beginning of September (phase 4) which is not followed by an emission increase that would be expected from

the early season responses (see Fig. 3), and (iii) the dramatic change in SEF of the mean of terpenoids and their derivatives (MTs, oMTs, m/z 153, SQTs, m/z 225), calculated for the flowering phase and fruit development/ ripening.

Seasonality, defined as long-term (cumulative) environmental conditions, explained and described some, but not all, of the temporal dynamics of the BVOC fluxes. Seasonal changes of MT and SQT emissions reflect changes of transcript, protein levels, availability of substrates for their biosynthesis, and enzyme activities involved in their biosynthesis (Fischbach *et al.*, 2002; Mayrhofer *et al.*, 2005; Ghirardo *et al.*, 2014; Wright *et al.*, 2014). While the cellular biochemistry is affected by the past weather conditions (Monson *et al.*, 2012), we could neither explain the large terpenoid emissions observed during the flowering phase, nor the sensitivity of other VOCs to high radiation phases during the ripening stage by means of the seasonal development factor.

One possible explanation is the presence of other influences that enhance BVOC emissions during the
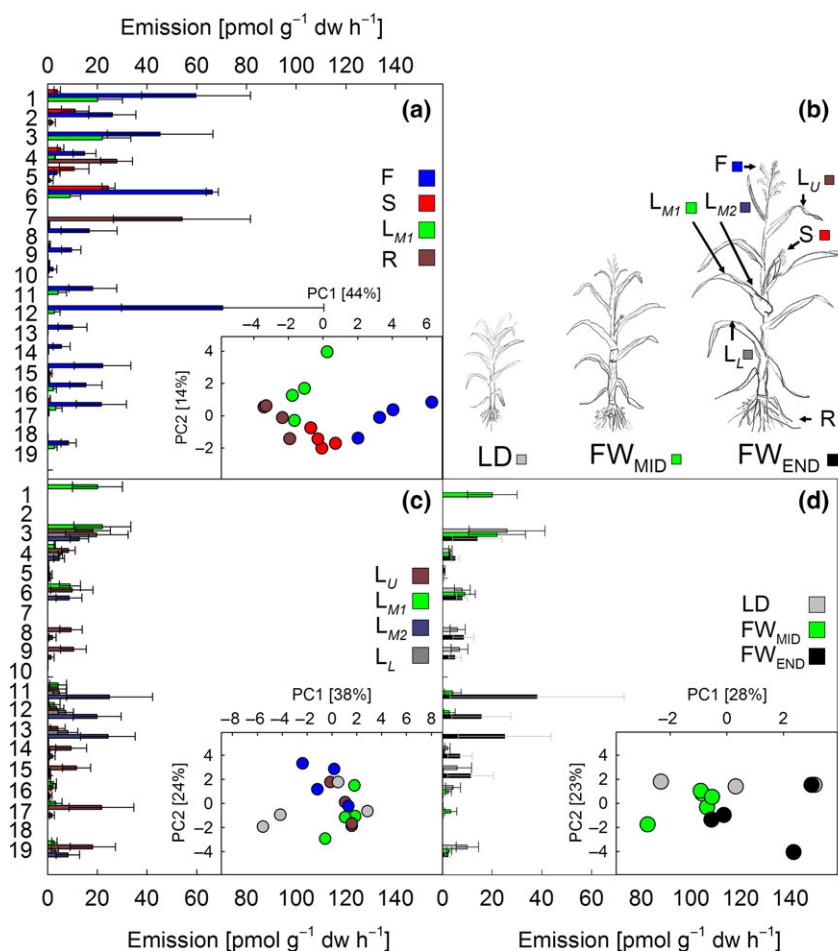
Fig. 5 Terpenoid emission rates from: (a) the plant tissues stigmata (S), male flower (F), leaf (L), and root (R); (c) young (L_U; upper leaf), mature (L_{M1}, L_{M2}), and old (L_L; lower leaf) leaves; (d) the phenological stage leaf development (L_D), mid (FW_{MID}) and end (FW_{END}) of the flowering phase (means of $N = 4 \pm$ standard error). The origin of the samples is schematically depicted in (b). Inserts: Principal component analysis (PCA) of the respective sample set. Compounds: 1 limonene; 2 1,8-cineole; 3 (E)-4,8-dimethyl-1,3,7-nona-triene; 4 camphor; 5 (E)-2-caren-4-ol; 6 decanal; 7 4-ethylguaiacol; 8 α-ylangene; 9 cyclosativene; 10 β-cubebene; 11 β-caryophyllene; 12 (E)-α-bergamotene; 13 (E)-β-farnesene; 14 α-humulene; 15 β-bisabolene; 16 γ-cadinene; 17 β-sesquiphellandrene; 18 (E)-nerolidol; 19 τ-cadinol. Further information can be found in Table S1.

flowering period. Our laboratory results indicate that flowering tissues are a strong source of terpenoids. This observation agrees well with previous studies on maize showing the tissue- and developmental stage-specific expression of terpene synthase genes in maize (Köllner *et al.*, 2004a,b). In accordance with the observations of Köllner and colleagues, we argue that terpenoids originating from the husks of the maize kernels further contributed significantly to the high observed fluxes of MTs and SQTs.

By applying the two different methods of normalizing and calculating SEFs for different growth periods, we could differentiate the compounds according by their temporal flux pattern into three groups: (i) terpenoids (MT, oMT, SQT) and their derivatives (*m/z* 153, *m/z* 225) with strongly differing SEF between the growth stages

and decreasing normalized emission rates from flowering to fruit development; (ii) methanol and ethanol showing an irregular SEF as well as emission and deposition flux pattern with strong relations to humidity; and (iii) other VOCs (fatty acids derivatives, ketones, aldehydes, and aromatics) with similar SEFs in all plant growth stages and decreasing normalized emission rates. Whereas the dynamics of terpenoids are explained by seasonal weather development and modified by phenological stages, the emissions of other VOCs strictly follow instantaneous temperature and radiation conditions. Moreover, the net fluxes for methanol and ethanol are difficult to reproduce without considering deposition fluxes that depend on air humidity or the occurrence of water on leaf surfaces. As methanol and ethanol fluxes changed from net

Table 3 Fitted standard emission factors (SEF) with corresponding standard errors of the estimate (SE) both in µg m^{-2} h^{-1}, fitted and standard value of the empirical β-coefficient from the equation for temperature-dependent emissions in K^{-1} (see Guenther, 1997) and coefficient of determination (R^2). SEF values are also calculated as a mean value for the three compound groups: terpenes, methanol, and ethanol, and other VOCs. All values are calculated for three growth periods flowering (FW, N = 495), fruit development and ripening (FR, N = 591), and the whole season (WS, N = 1110)

Compound	Period	SEF (± SE)	β	R^2	SEF (± SE)	β	R^2
m/z 69*	FW	39.24 (± 5.45)	-	0.82	-	-	-
	FR	30.49 (± 2.96)	-	0.77	-	-	-
	WS	36.73 (± 4.47)	-	0.82	-	-	-
MTs*	FW	254.2 (± 35.16)	-	0.85	-	-	-
	FR	184.84 (± 15.02)	-	0.85	-	-	-
	WS	235.36 (± 27.93)	-	0.85	-	-	-
m/z 69	FW	29.72 (± 6.52)	0.09	0.75	33.78 (± 4.98)	0.135	0.85
	FR	16.79 (± 4.23)	0.09	0.53	31.21 (± 3.31)	0.171	0.71
	WS	24.67 (± 6.15)	0.09	0.65	32.3 (± 4.41)	0.152	0.82
MTs	FW	177.74 (± 58.32)	0.09	0.6	207.09 (± 48.91)	0.146	0.72
	FR	93.85 (± 28.12)	0.09	0.47	202.34 (± 20.66)	0.191	0.72
	WS	145.43 (± 48.51)	0.09	0.54	198.66 (± 37.47)	0.162	0.72
m/z 153	FW	59.77 (± 23.07)	0.09	0.55	73.57 (± 15.89)	0.183	0.79
	FR	20.35 (± 5.37)	0.09	0.53	44.05 (± 3.52)	0.193	0.8
	WS	44.44 (± 18.27)	0.09	0.46	67.28 (± 11.69)	0.203	0.78
oMTs	FW	15.67 (± 5.33)	0.09	0.61	19.11 (± 3.49)	0.174	0.83
	FR	9.95 (± 3.3)	0.09	0.44	22.43 (± 2.47)	0.197	0.68
	WS	13.47 (± 4.54)	0.09	0.55	19.25 (± 3.01)	0.177	0.8
SQTs	FW	57.28 (± 16.61)	0.09	0.66	68.41 (± 10.81)	0.166	0.86
	FR	16.66 (± 4.72)	0.09	0.5	36.61 (± 3.22)	0.195	0.77
	WS	41.86 (± 14.78)	0.09	0.52	61.46 (± 8.99)	0.193	0.82
m/z 225	FW	0.82 (± 0.29)	0.09	0.58	0.99 (± 0.22)	0.165	0.76
	FR	0.14 (± 0.07)	0.09	0.22	0.27 (± 0.07)	0.17	0.3
	WS	0.56 (± 0.25)	0.09	0.41	0.84 (± 0.18)	0.201	0.68
Mean	**FW**	**113.52**	**0.09**	-	-	-	-
Terpenoids†	**FR**	**60.47**	**0.09**	-	-	-	-
	WS	**92.7**	**0.09**	-	-	-	-
Methanol	FW	32.65 (± 34.35)	0.09	0.2	45.88 (± 30.46)	0.215	0.37
	FR	18.45 (± 19.5)	0.09	0.1	53.32 (± 18.4)	0.218	0.2
	WS	25.14 (± 28.5)	0.09	0.14	44.96 (± 25.71)	0.221	0.3
Ethanol	FW	3.14 (± 7.01)	0.09	0.05	6.07 (± 6.1)	0.293	0.28
	FR	5.38 (± 9.42)	0.09	0.05	18.82 (± 9.02)	0.215	0.13
	WS	3.75 (± 8.45)	0.09	0.04	8.18 (± 8.04)	0.23	0.13
Mean	**FW**	**30.8**	**0.09**	-	-	-	-
Methanol and	**FR**	**16.25**	**0.09**	-	-	-	-
Ethanol	**WS**	**23.13**	**0.09**	-	-	-	-
Acetaldehyde	FW	41.05 (± 9.89)	0.09	0.71	46.22 (± 8.31)	0.131	0.8
	FR	31.65 (± 10.26)	0.09	0.42	57.76 (± 8.92)	0.167	0.56
	WS	37.19 (± 10.37)	0.09	0.6	46.78 (± 8.82)	0.14	0.71
Acetone	FW	57.29 (± 16.79)	0.09	0.66	67.37 (± 12.68)	0.152	0.8
	FR	55.1 (± 15.44)	0.09	0.49	104.28 (± 12.45)	0.173	0.67
	WS	56.23 (± 16.16)	0.09	0.59	72.45 (± 13.27)	0.146	0.72
m/z 71	FW	17.45 (± 6.82)	0.09	0.56	21.55 (± 4.69)	0.183	0.79
	FR	12.38 (± 5.66)	0.09	0.29	26.16 (± 5.04)	0.186	0.44
	WS	15.3 (± 6.39)	0.09	0.45	22.07 (± 4.99)	0.179	0.67
Hexenal	FW	36.47 (± 12.53)	0.09	0.61	44.7 (± 7.96)	0.176	0.84
	FR	35.87 (± 12.52)	0.09	0.4	71.89 (± 10.58)	0.18	0.57
	WS	36.13 (± 12.57)	0.09	0.52	49.16 (± 10.06)	0.161	0.69
Hexanal	FW	93.7 (± 34.41)	0.09	0.58	114.74 (± 24.26)	0.171	0.79

(continued)

Table 3 (continued)

Compound	Period	SEF (± SE)	β	R^2	SEF (± SE)	β	R^2
	FR	94.7 (± 34.52)	0.09	0.39	205.21 (± 28.23)	0.191	0.59
	WS	93.74 (± 34.76)	0.09	0.49	127.66 (± 28.57)	0.16	0.66
Xylenes	FW	10.69 (± 3.91)	0.09	0.57	12.77 (± 3.14)	0.158	0.72
	FR	13.53 (± 4.79)	0.09	0.39	26.04 (± 4.16)	0.174	0.54
	WS	11.74 (± 4.46)	0.09	0.46	14.9 (± 4.07)	0.141	0.55
DMNT	FW	25.69 (± 8.55)	0.09	0.6	30.35 (± 6.84)	0.153	0.75
	FR	20.72 (± 8.6)	0.09	0.31	37.09 (± 7.98)	0.164	0.4
	WS	23.76 (± 8.66)	0.09	0.48	31.25 (± 7.51)	0.151	0.61
Mean	**FW**	**54.94**	**0.09**	-	-	-	-
Other VOCs	**FR**	**53.93**	**0.09**	-	-	-	-
	WS	**54.19**	**0.09**	-	-	-	-

*SEFs are calculated by Eqn (3), depending on both, temperature, and radiation.

†SEF values from m/z 69 and MTs are included only from temperature dependent equation.

Average emission factors for the whole group are indicated in bold.

ecosystem emission to net deposition during or after precipitation events, it is very likely that this behaviour is affected by the high water solubility of the compounds (Niinemets *et al.*, 2004). In dry periods, however, methanol emissions seemed to develop similar to those of other VOCs, indicating a temperature dependency related to biological processes and their biosynthesis as has been recently pointed out by Mozaffar *et al.* (2017). Whereas ethanol emissions are the results of alcoholic sugar fermentation generally originating from roots (Kreuzwieser *et al.*, 1999).

We also found a strong similarity ($R^2 = 0.94$) between normalized fluxes from m/z 69 and MTs. The TD-GC-MS analysis could not identify m/z 69 as isoprene, but traces of pentanal, octanal, nonanal, and decanal could be detected. These fatty aldehydes, which are typical natural products used in fragrance and flavour production, all fragment into m/z 69 (e.g. Schwarz *et al.*, 2009). The diurnal cycle of MTs implies that also maize MTs originate from *de novo* biosynthesis, which agrees with the observation of Köllner *et al.* (2004a). For the same reason, the origin of SQTs is assumed to be *de novo*. The stronger decrease of m/z 153 and SQTs compared to m/z 69, MTs, and oMTs in phase 3, coincides with the ending of the flowering phase. This can be explained by completely dried stigmata and completed male flowering when flowering phase ends, as those tissues emit camphor, (*E*)-2-caren-4-ol (summed in m/z 153), and SQTs to a large extent (see Fig. 5a).

Beside instantaneous temperature and radiation constrains, we believe that also cumulative weather and plant ontogenesis influenced the temporal dynamics of BVOC fluxes. We could not find any evidence of pest infestation during the field campaign, although we cannot exclude that to some extent changes in m/z 153 (especially methyl salicylate), oMTs, and SQTs are due to herbivorous attacks. Induced or reduced emissions due to heat or drought stress are unlikely, given the fact that NEE was not impaired during the warmest periods and that soil water availability was never in demand (data not shown).

Comparison with other BVOC emission studies on maize

So far only a few studies have analysed BVOC fluxes from maize canopies. These include some investigation with GC-MS analyses during a field campaign in Germany (Wedel *et al.*, 1998) and some short-term investigations by Das *et al.* (2003) and Graus *et al.* (2013). The only extensive field study was performed by Bachy *et al.* (2016) followed up by the recent work of Mozaffar *et al.* (2017) who measured two cultivars for each phenological developmental stage. Generally, all studies have in common that BVOC emissions showed a large diurnal and daily variability similar to the present work. However, the distinct compound classes, in particular the group of SQTs has neither been depicted nor analysed before.

It should be noted, however, that comparison of SEFs depends on the collection of BVOC data as well as the equation parameters. For example, here we have shown that fitting both SEF and β-coefficients leads to a better result with smaller standard error and higher R^2 values. As all fitted β-coefficients are higher than the empirical mean value of 0.09 (Guenther *et al.*, 1993; Guenther, 1997) also the SEF values become higher compared to a fit with constant β. In this context, it is important to note that, using the standard β-coefficient of Guenther *et al.* (1993, Guenther, 1997) might result in an underestimation of BVOC fluxes from maize (or other crops as well). In contrast, methanol and ethanol fluxes might become overestimated if SEFs are developed from data collected

during warm and dry weather periods alone, because the importance of deposition processes during wet periods has been neglected.

To compare our results with those from the different studies, we are concentrating on the flowering period and calculate all emission data as µg m^{-2} ground area h^{-1}. We found that the most abundant emissions from this period were methanol, MTs, GLVs, acetaldehyde, and acetone ranging from 13% to 18% of the total molar BVOC fluxes. In absolute terms, the mean methanol emission rate is 4 µg m^{-2} h^{-1} (mean of positive and negative fluxes), which is considerable smaller than what has been found by Bachy *et al.* (2016) ($\sim$50 µg m^{-2} h^{-1}), Graus *et al.* (2013) (400 µg m^{-2} h^{-1}), or Das *et al.* (2003) (3450 µg m^{-2} h^{-1}). Also MT and acetone emissions (65 and 21 µg m^{-2} h^{-1}, respectively) are more than one magnitude lower compared to Das *et al.* (2003) (661 and 425 µg m^{-2} h^{-1}, respectively) but are higher than has been reported by Graus *et al.* (2013) ($\sim$50 µg m^{-2} h^{-1}) and Bachy *et al.* (2016) ($\sim$2 µg m^{-2} h^{-1}). GLVs were only detected by Graus *et al.* (2013) and Wedel *et al.* (1998). In summary, we observed higher emission rates than obtained by Bachy *et al.* (2016), for all compounds except for methanol, while they are generally lower when compared to the results from Das *et al.* (2003) and Graus *et al.* (2013). However, it should be considered that at least the latter work reported only midday fluxes and fluxes under environmental standard conditions.

The SEF for MTs for the whole season is 145 µg m^{-2} h^{-1} if we assume temperature dependence only and 235 µg m^{-2} h^{-1} if the flux is assumed to be temperature and radiation dependent (see Table 3). Both values are of similar magnitude compared to other bioenergy crop systems such as oil palm (SEF of 102–113 µg m^{-2} h^{-1}) and eucalyptus (200–600 µg m^{-2} h^{-1}) (Rosenkranz *et al.*, 2015). Additionally, we observed a whole array of substances including significant emissions of SQTs for which flux rates over maize fields were previously not detected. SQTs are considered to be a very important precursor for SOA, already at relatively low concentrations (Bonn & Moortgat, 2003; Mentel *et al.*, 2013). Given the much higher abundance of maize fields than short rotation coppices in most parts of the world, the present data highlights the importance for estimates from agricultural sides to assess regional air quality and regional climate.

Overall, the investigation adds to the large variability found in different studies, which can be only partially explained with methodological differences. As maize fields are carried out with a lot of different cultivars, differences in genotypes may also explain part of the variation (Gouinguené *et al.*, 2001), underlining the need for a systematic screening of cultivars.

Suitability of automatic chamber measurements

Using large automatic chambers for measuring maize canopy BVOC fluxes have shown several advantages. First, the closed chamber method enabled measuring absolute fluxes of many volatiles including SQTs, *m/z* 153, and oMTs, which were not observed or at least not quantified in previous maize field experiments. In particularly, the volatile SQTs were hardly detectable at canopy scale (Ciccioli *et al.*, 1999; Jardine *et al.*, 2011), although they are supposed to play an important role in aerosol formation (e.g. Hallquist *et al.*, 2009; Li *et al.*, 2011). The investigation thus confirms previous genetic and physiological investigation on tissue level which already indicated that both SQTs and oMTs are potentially emitted by maize in considerable quantities (Schnee *et al.*, 2002, 2006; Köllner *et al.*, 2004a,b; Fontana *et al.*, 2011). A second advantage of the present chamber approach is the fact that a defined ecosystem patch is measured, which on the one hand can be assumed as representative and on the other can be easily defined (in terms of number of individuals, height, LAI, phenological stage).

Nevertheless, a number of precautions need to be carefully taken into account to avoid erroneous data collection and reduce uncertainties. In particular at days with strong radiation, the 'greenhouse effect' within the chamber may lead to rising temperatures and the strong assimilation decreases CO_2 concentrations and increases relative humidity, which both potentially affect BVOC emissions and deposition. For security reasons, chambers open automatically when a temperature threshold of about 40 °C is exceeded, which has not been reached during the investigations (observed maximum of 38.7 °C). Within this limit, we argue that not only temperature changes but also variations in CO_2 concentration are not affecting the *de novo* synthesis of BVOCs within 12 min (i.e. the period of chamber closure) (Noe *et al.*, 2010). Thus, only emissions from storages that do not directly originate from *de novo* production but depend on storage size and evaporation resistance could still be influenced (Ghirardo *et al.*, 2010; Peñuelas & Staudt, 2010), which we checked using laboratory experiments. These exercises showed no BVOC emission increase within 12 min for changes in temperature and CO_2 concentrations that were similar to the highest ones observed during the field campaign (data not shown). As we could not detect strong nonlinearities of BVOC concentration changes within the chambers, we assume that the share of storage-based emission is either small (in agreement with Köllner *et al.*, 2004a) or that the change in headspace temperature was unable to increase tissue temperature during chamber closure.

Another source of uncertainty is the possible reaction of BVOCs with atmospheric NO_x, OH, and O_3 inside the chamber, which may occur particularly if radiation and temperature are high. We have no indication about OH (pptv) concentrations but assume that they are generally low at the remote site, which is not much affected by anthropogenic emissions. The remaining reactivity depends on the relation of BVOCs to NO and O_3 concentrations. NO originates mainly from soil emissions (Pilegaard, 2013) which are continuously fuelling air concentrations and thus are likely to be relatively high in comparison with background levels of O_3 (usually 10–40 ppb according to Atkinson & Arey, 2003). Therefore, chemical reactions of BVOCs are unlikely because NO molecules will react with O_3 quite fast producing NO_2 and depleting O_3 quickly. This is supported by the linear increase of BVOC emissions, indicating no or minor secondary reactions between BVOC and inorganic components of the atmosphere. Thus, the simple linear regression approach seems suitable to retrieve reliable trace gas exchange rates for BVOCs.

Despite some uncertainties that remain to be investigated in future studies, the overall approach is likely to be applicable to other crop species as well. As the chambers can be temporally removed from the ground, different kinds of management can also been applied and investigated. Together, this makes the method potentially interesting for comparative studies in preparation for extrapolating the results to the regional scale.

Acknowledgements

Competing financial interests

The authors declare no competing financial interests exist.

References

Arbeitsgemeinschaft Energiebilanzen (2015) Auswertungstabellen zur Energiebilanz Deutschland. 1990 bis 2014. Tech. rep., Arbeitsgemeinschaft Energiebilanzen e.V.

Ashworth K, Wild O, Hewitt C (2013) Impacts of biofuel cultivation on mortality and crop yields. *Nature Climate Change*, **3**, 492–496.

Atkinson R, Arey J (2003) Gas-phase tropospheric chemistry of biogenic volatile organic compounds: a review. *Atmospheric Environment*, **37**, 197–219.

Bachy A, Aubinet M, Schoon N, Amelynck C, Bodson B, Moureaux C, Heinesch B (2016) Are BVOC exchanges in agricultural ecosystems overestimated? Insights from fluxes measured in a maize field over a whole growing season. *Atmospheric Chemistry and Physics*, **16**, 5343–5356.

Beltman JB, Hendriks C, Tum M, Schaap M (2013) The impact of large scale biomass production on ozone air pollution in Europe. *Atmospheric Environment*, **71**, 352–363.

Bentsen NS, Felby C (2012) Biomass for energy in the European Union - a review of bioenergy resource assessments. *Biotechnology for Biofuels*, **5**, 1–10.

Bonn B, Moortgat GK (2003) Sesquiterpene ozonolysis: origin of atmospheric new particle formation from biogenic hydrocarbons. *Geophysical Research Letters*, **30**, 1585–1588.

Brilli F, Ruuskanen TM, Schnitzhofer R *et al.* (2011) Detection of plant volatiles after leaf wounding and darkening by proton transfer reaction "time-of-flight" mass spectrometry (PTR-TOF). *PLoS ONE*, **6**, 1–12.

Calfapietra C, Fares S, Manes F, Morani A, Sgrigna G, Loreto F (2013) Role of Biogenic Volatile Organic Compounds (BVOC) emitted by urban trees on ozone concentration in cities: a review. *Environmental Pollution*, **183**, 71–80.

Capros P, De Vita A, Tasios N *et al.* (2014) *EU Energy, Transport and GHG Emissions Trends to 2050 – Reference Scenario 2013*. Publications Office of the European Union, Luxembourg.

Ciccioli P, Brancaleoni E, Frattoni M (1999) Emission of reactive terpene compounds from orange orchards and their removal by within-canopy processes. *Journal of Geophysical Research*, **104**, 8077–8094.

Crutzen PJ, Mosier AR, Smith KA, Winiwarter W (2008) N_2O release from agrobiofuel production negates global warming reduction by replacing fossil fuels. *Atmospheric Chemistry and Physics*, **8**, 389–395.

Das M, Kang D, Aneja V, Lonneman W, Cook D, Wesely M (2003) Measurements of hydrocarbon air–surface exchange rates over maize. *Atmospheric Environment*, **37**, 2269–2277.

Davidson EA, Savage K, Verchot LV, Navarro R (2002) Minimizing artifacts and biases in chamber-based measurements of soil respiration. *Agricultural and Forest Meteorology*, **113**, 21–37.

Erneuerbare-Energien-Gesetz (2014) *Erneuerbare-Energien-Gesetz - EEG 2014*. Gesetz für den Ausbau erneuerbarer Energien.

European Union (2014) *State of play on the sustainability of solid and gaseous biomass used for electricity, heating and cooling in the EU*. European Commission, Commission staff working document, Brussels.

Fachagentur für Nachwachsende Rohstoffe (2016) Homepage. Available at: http://www.fnr.de (accessed 28 July 2016).

Fischbach RJ, Staudt M, Zimmer I, Rambal S, Schnitzler JP (2002) Seasonal pattern of monoterpene synthase activities in leaves of the evergreen tree *Quercus ilex*. *Physiologia Plantarum*, **114**, 354–360.

Fontana A, Held M, Fantaye CA, Turlings TC, Degenhardt J, Gershenzon J (2011) Attractiveness of constitutive and herbivore-induced sesquiterpene blends of maize to the parasitic wasp *Cotesia marginiventris* (cresson). *Journal of Chemical Ecology*, **37**, 582.

Ghirardo A, Koch K, Taipale R, Zimmer I, Schnitzler JP, Rinne J (2010) Determination of de novo and pool emissions of terpenes from four common boreal/alpine trees by $^{13}CO_2$ labelling and PTR-MS analysis. *Plant, Cell and Environment*, **33**, 781–792.

Ghirardo A, Gutknecht J, Zimmer I, Brüggemann N, Schnitzler JP (2011) Biogenic volatile organic compound and respiratory CO_2 emissions after ^{13}C-labeling: online tracing of C translocation dynamics in poplar plants. *PLoS ONE*, **6**, e17393.

Ghirardo A, Heller W, Fladung M, Schnitzler JP, Schroeder H (2012) Function of defensive volatiles in pedunculate oak (*Quercus robur*) is tricked by the moth *Tortrix viridana*. *Plant, Cell and Environment*, **35**, 2192–2207.

Ghirardo A, Wright LP, Bi Z *et al.* (2014) Metabolic flux analysis of plastidic isoprenoid biosynthesis in poplar leaves emitting and nonemitting isoprene. *Plant Physiology*, **165**, 37–51.

Ghirardo A, Xie J, Zheng X *et al.* (2016) Urban stress-induced biogenic VOC emissions and SOA-forming potentials in Beijing. *Atmospheric Chemistry and Physics*, **16**, 2901–2920.

Gouinguené S, Degen T, Turlings TCJ (2001) Variability in herbivore-induced odour emissions among maize cultivars and their wild ancestors (teosinte). *Chemoecology*, **11**, 9–16.

Graus M, Eller A, Fall R *et al.* (2013) Biosphere-atmosphere exchange of volatile organic compounds over C4 biofuel crops. *Atmospheric Environment*, **66**, 161–168.

Guenther A (1997) Seasonal and spatial variations in natural volatile organic compound emissions. *Ecological Applications*, **7**, 34–45.

Guenther AB, Zimmerman PR, Harley PC, Monson RK, Fall R (1993) Isoprene and monoterpene emission rate variability: model evaluations and sensitivity analyses. *Journal of Geophysical Research*, **98**, 12609–12617.

Guenther A, Karl T, Harley P, Wiedinmyer C, Palmer PI, Geron C (2006) Estimates of global terrestrial isoprene emissions using megan (model of emissions of gases and aerosols from nature). *Atmospheric Chemistry and Physics*, **6**, 3181–3210.

Hallquist M, Wenger JC, Baltensperger U *et al.* (2009) The formation, properties and impact of secondary organic aerosol: current and emerging issues. *Atmospheric Chemistry and Physics*, **9**, 5155–5236.

Hansel A, Jordan A, Warneke C, Holzinger R, Wisthaler A, Lindinger W (1999) Proton-transfer-reaction mass spectrometry (PTR-MS): on-line monitoring of volatile organic compounds at volume mixing ratios of a few pptv. *Plasma Sources Science and Technology*, **8**, 332.

Hoffmann M, Jurisch N, Albiac Borraz E, Hagemann U, Drösler M, Sommer M, Augustin J (2015) Automated modeling of ecosystem CO_2 fluxes based on periodic closed chamber measurements: a standardized conceptual and practical approach. *Agricultural and Forest Meteorology*, **200**, 30–45.

Hoffmann M, Jurisch N, Garcia Alba J *et al.* (2016) Detecting small-scale spatial heterogeneity and temporal dynamics of soil organic carbon (SOC) stocks: a comparison between automatic chamber-derived C budgets and repeated soil inventories. *Biogeosciences Discussions*, **2016**, 1–45.

Immerzeel DJ, Verweij PA, van der Hilst F, Faaij APC (2014) Biodiversity impacts of bioenergy crop production: a state-of-the-art review. *GCB Bioenergy*, **6**, 183–209.

International Energy Agency (2015) *Excerpt From Renewables Information – IEA Statistics: Key Renewables Trends*. International Energy Agency. Licence: wwwi.iea.org/t&c.

Jardine K, Yanez Serrano A, Arneth A, et al. (2011) Within-canopy sesquiterpene ozonolysis in Amazonia. *Journal of Geophysical Research*, **116**, D19301.

Kesselmeier J, Staudt M (1999) Biogenic Volatile Organic Compounds (VOC): an overview on emission, physiology and ecology. *Journal of Atmospheric Chemistry*, **33**, 23–88.

Köllner TG, Schnee C, Gershenzon J, Degenhardt J (2004a) The sesquiterpene hydrocarbons of maize (*Zea mays*) form five groups with distinct developmental and organ-specific distributions. *Phytochemistry*, **65**, 1895–1902.

Köllner TG, Schnee C, Gershenzon J, Degenhardt J (2004b) The variability of sesquiterpenes emitted from two *Zea mays* cultivars is controlled by allelic variation of two terpene synthase genes encoding stereoselective multiple product enzymes. *The Plant Cell*, **16**, 1115–1131.

Kreuzwieser J, Scheerer U, Rennenberg H (1999) Metabolic origin of acetaldehyde emitted by poplar (*Populus tremula × P. alba*) trees. *Journal of Experimental Botany*, **50**, 757.

Kreuzwieser J, Scheerer U, Kruse J *et al.* (2014) The venus flytrap attracts insects by the release of volatile organic compounds. *Journal of Experimental Botany*, **65**, 755–766.

Kutzbach L, Schneider J, Sachs T *et al.* (2007) CO_2 flux determination by closed-chamber methods can be seriously biased by inappropriate application of linear regression. *Biogeosciences*, **4**, 1005–1025.

Langensiepen M, Kupisch M, van Wijk MT, Ewert F (2012) Analyzing transient closed chamber effects on canopy gas exchange for flux calculation timing. *Agricultural and Forest Meteorology*, **164**, 61–70.

Leiber-Sauheitl K, Fuß R, Voigt C, Freibauer A (2014) High CO_2 fluxes from grassland on histic Gleysol along soil carbon and drainage gradients. *Biogeosciences*, **11**, 749–761.

Leifeld J, Ammann C, Neftel A, Fuhrer J (2011) A comparison of repeated soil inventory and carbon flux budget to detect soil carbon stock changes after conversion from cropland to grasslands. *Global Change Biology*, **17**, 3366–3375.

Leppik E, Tammaru T, Frérot B (2014) A view of diel variation of maize odorscape. *American Journal of Plant Sciences*, **5**, 811–820.

Li YJ, Chen Q, Guzman MI, Chan CK, Martin ST (2011) Second-generation products contribute substantially to the particle-phase organic material produced by β-caryophyllene ozonolysis. *Atmospheric Chemistry and Physics*, **11**, 121–132.

Lindinger W, Hansel A, Jordan A (1998) On-line monitoring of volatile organic compounds at pptv levels by means of proton-transfer-reaction mass spectrometry (PTR-MS) medical applications, food control and environmental research. *International Journal of Mass Spectrometry and Ion Processes*, **173**, 191–241.

Loreto F, Ciccioli P, Brancaleoni E, Frattoni M, Delfine S (2000) Incomplete 13C labelling of α-pinene content of *Quercus ilex* leaves and appearance of unlabelled C in α-pinene emission in the dark. *Plant, Cell and Environment*, **23**, 229–234.

Makkonen R, Asmi A, Kerminen VM, Boy M, Arneth A, Guenther A, Kulmala M (2012) BVOC-aerosol-climate interactions in the global aerosol-climate model ECHAM5.5-HAM2. *Atmospheric Chemistry and Physics*, **12**, 10077–10096.

Mayrhofer S, Teuber M, Zimmer I, Louis S, Fischbach RJ, Schnitzler JP (2005) Diurnal and seasonal variation of isoprene biosynthesis-related genes in grey poplar leaves. *Plant Physiology*, **139**, 474–484.

Meier U, ed. (2001) *Growth stages of mono-and dicotyledonous pants. BBCH Monograph*. Federal Biological Research Center for Agriculture and Forestry, 2nd edn. Blackwell, Boston

Mentel TF, Kleist E, Andres S *et al.* (2013) Secondary aerosol formation from stress-induced biogenic emissions and possible climate feedbacks. *Atmospheric Chemistry and Physics*, **13**, 8755–8770.

Miresmailli S, Zeri M, Zangerl AR, Bernacchi CJ, Berenbaum MR, DeLucia EH (2013) Impacts of herbaceous bioenergy crops on atmospheric volatile organic composition and potential consequences for global climate change. *GCB Bioenergy*, **5**, 375–383.

Monson RK, Grote R, Niinemets Ü, Schnitzler JP (2012) Modeling the isoprene emission rate from leaves. *New Phytologist*, **195**, 541–559.

Morrison EC, Drewer J, Heal MR (2016) A comparison of isoprene and monoterpene emission rates from the perennial bioenergy crops short-rotation coppice willow and *Miscanthus* and the annual arable crops wheat and oilseed rape. *GCB Bioenergy*, **8**, 211–225.

Mozaffar A, Schoon N, Digrado A *et al.* (2017) Methanol emissions from maize: ontogenetic dependence to varying light conditions and guttation as an additional factor constraining the flux. *Atmospheric Environment*, **152**, 405–417.

Niinemets Ü, Loreto F, Reichstein M (2004) Physiological and physicochemical controls on foliar volatile organic compound emissions. *Trends in Plant Science*, **9**, 180–186.

Nikièma P, Rothstein DE, Miller RO (2012) Initial greenhouse gas emissions and nitrogen leaching losses associated with converting pastureland to short-rotation woody bioenergy crops in northern Michigan, USA. *Biomass and Bioenergy*, **39**, 413–426.

Noe S, Niinemets Ü, Schnitzler JP (2010) Modeling the temporal dynamics of monoterpene emission by isotopic labeling in *Quercus ilex* leaves. *Atmospheric Environment*, **44**, 392–399.

Peñuelas J, Staudt M (2010) BVOCs and global change. *Trends in Plant Science*, **15**, 133–144.

Pilegaard K (2013) Processes regulating nitric oxide emissions from soils. *Philosophical Transactions of the Royal Society of London B: Biological Sciences*, **368**, 20130126.

Pohl M, Hoffmann M, Hagemann U, Giebels M, Albiac Borraz E, Sommer M, Augustin J (2015) Dynamic C and N stocks - key factors controlling the C gas exchange of maize in heterogenous peatland. *Biogeosciences*, **12**, 2737–2752.

Porter WC, Barsanti KC, Baughman EC, Rosenstiel TN (2012) Considering the air quality impacts of bioenergy crop production: a case study involving *Arundo donax*. *Environmental Science and Technology*, **46**, 9777–9784.

Portillo-Estrada M, Kazantsev T, Talts E, Tosens T, Niinemets Ü (2015) Emission timetable and quantitative patterns of wound-induced volatiles across different leaf damage treatments in aspen (*Populus tremula*). *Journal of Chemical Ecology*, **41**, 1105–1117.

Renner E, Münzenberg A (2003) Impact of biogenic terpene emissions from *Brassica napus* on tropospheric ozone over saxony (Germany). *Environmental Science and Pollution Research*, **10**, 147–153.

Richter A, Schaff C, Zhang Z *et al.* (2016) Characterization of biosynthetic pathways for the production of the volatile homoterpenes DMNT and TMTT in *Zea mays*. *The Plant Cell*, **28**, 2651–2665.

Rosenkranz M, Pugh TAM, Schnitzler JP, Arneth A (2015) Effect of land-use change and management on BVOC emissions – selecting climate-smart cultivars. *Plant Cell and Environment*, **38**, 1896–1912.

Schnee C, Köllner TG, Gershenzon J, Degenhardt J (2002) The Maize gene terpene synthase 1 encodes a sesquiterpene synthase catalyzing the formation of (E)-β-farnesene, (E)-nerolidol, and (E, E)-farnesol after herbivore damage. *Plant Physiology*, **130**, 2049–2060.

Schnee C, Köllner TG, Held M, Turlings TCJ, Gershenzon J, Degenhardt J (2006) The products of a single maize sesquiterpene synthase form a volatile defense signal that attracts natural enemies of maize herbivores. *Proceedings of the National Academy of Sciences of the United States of America*, **103**, 1129–1134.

Schultz MG, Akimoto H, Bottenheim J *et al.* (2015) The global atmosphere watch reactive gases measurement network. *Elementa: Science of the Anthropocene*, **3**, 67.

Schwarz K, Filipiak W, Amann A (2009) Determining concentration patterns of volatile compounds in exhaled breath by PTR-MS. *Journal of Breath Research*, **3**, 027002.

Sommer M, Augustin J, Kleber M (2016) Feedbacks of soil erosion on SOC patterns and carbon dynamics in agricultural landscapes—the CarboZALF experiment. *Soil and Tillage Research*, **156**, 182–184.

Tarvainen V, Hakola H, Hellén H, Bäck J, Hari P, Kulmala M (2005) Temperature and light dependence of the VOC emissions of Scots pine. *Atmospheric Chemistry and Physics*, **5**, 989–998.

Wedel A, Müller K-P, Ratte M, Rudolph J (1998) Measurements of Volatile Organic Compounds (VOC) during POPCORN 1994: applying a new on-line GC-MS-technique. In: *Atmospheric Measurements during POPCORN — Characterisation of the Photochemistry over a Rural Area* (eds Rudolph J, Koppmann R), pp. 73–103. Springer Netherlands, Dordrecht.

Weikl F, Ghirardo A, Schnitzler JP, Pritsch K (2016) Sesquiterpene emissions from *Alternaria alternata* and *Fusarium oxysporum*: effects of age, nutrient availability, and co-cultivation. *Scientific Reports*, **6**, 22152.

Wright LP, Rohwer JM, Ghirardo A *et al.* (2014) Deoxyxylulose 5-phosphate synthase controls flux through the methylerythritol 4-phosphate pathway in *Arabidopsis*. *Plant Physiology*, **165**, 1488–1504.

Supporting Information

Additional Supporting Information may be found online in the supporting information tab for this article:

Table S1. Chemical identification of BVOCs and calculated Kovats' retention index.
Figure S1. Principal component analysis of all BVOC data from different maize tissues collected under controlled laboratory conditions.